

Simulation of DNA Electrophoresis in Systems of Large Number of Solvent Particles by Coarse-Grained Hybrid Molecular Dynamics Approach

RONG WANG,^{1,2} JIAN-SHENG WANG,^{2,3} GUI-RONG LIU,^{2,4} JONGYOON HAN,^{2,5} YU-ZONG CHEN^{2,6}

¹Department of Polymer Science and Engineering, Nanjing National Laboratory of Microstructures, School of Chemistry and Chemical Engineering, Nanjing University, Nanjing 210093, China

²Singapore-MIT Alliance, 4 Engineering Drive 3, Singapore 117576

³Department of Physics, National University of Singapore, 2 Science Drive 3, Singapore 117542

⁴Center for Advanced Computations in Engineering Science (ACES), Department of Mechanical Engineering, National University of Singapore, 9 Engineering Drive 1, Singapore 117576

⁵Department of Electrical Engineering and Computer Science, Department of Biological Engineering, Massachusetts Institute of Technology, Cambridge, Massachusetts 02139

⁶Department of Pharmacy, National University of Singapore, 8 Science Drive 4, Singapore 117543

Received 13 December 2007; Revised 14 May 2008; Accepted 24 June 2008

DOI 10.1002/jcc.21081

Published online 4 September 2008 in Wiley InterScience (www.interscience.wiley.com).

Abstract: Simulation of DNA electrophoresis facilitates the design of DNA separation devices. Various methods have been explored for simulating DNA electrophoresis and other processes using implicit and explicit solvent models. Explicit solvent models are highly desired but their applications may be limited by high computing cost in simulating large number of solvent particles. In this work, a coarse-grained hybrid molecular dynamics (CGH-MD) approach was introduced for simulating DNA electrophoresis in explicit solvent of large number of solvent particles. CGH-MD was tested in the simulation of a polymer solution and computation of nonuniform charge distribution in a cylindrical nanotube, which shows good agreement with observations and those of more rigorous computational methods at a significantly lower computing cost than other explicit-solvent methods. CGH-MD was further applied to the simulation of DNA electrophoresis in a polymer solution and in a well-studied nanofluidic device. Simulation results are consistent with observations and reported simulation results, suggesting that CGH-MD is potentially useful for studying electrophoresis of macromolecules and assemblies in nanofluidic, microfluidic, and microstructure array systems that involve extremely large number of solvent particles, nonuniformly distributed electrostatic interactions, bound and sequestered water molecules.

© 2008 Wiley Periodicals, Inc. J Comput Chem 30: 505–513, 2009

Key words: molecular dynamics; explicit solvent; coarse-grained; DNA electrophoresis; nanofluidic device

Introduction

Electrophoresis has been widely used for separating polyelectrolytes such as DNA and proteins.^{1–4} Significant progress has been made in developing simulation models of DNA and protein electrophoresis in nanofluidic devices and other systems primarily using implicit solvent methods. For example, the bond-fluctuation Monte-Carlo method has been used for simulating the motion of long polyelectrolytes inside an array of microscopic traps.⁵ The mobility of DNA and its length-dependent time scale of movement have been studied by Brownian dynamics (BD) simulations.^{6,7} These simulation studies have yielded good agreement with observations.^{8–11} However, some of the explicit

solvent effects such as nonuniformly distributed electrostatic interactions, hydrophobic effects, and bound and sequestered water molecules^{12,13} cannot be fully considered without using explicit solvent methods. As these effects play important roles in electrophoresis and other processes, it is highly desired to explore explicit solvent methods in practical applications.

Correspondence to: R. Wang; e-mail: rong_wang73@hotmail.com; or Y.-Z. Chen; e-mail: phacyz@nus.edu.sg

Grant sponsor: National Natural Science Foundation of China; grant numbers: 20504013, 20674035

Grant sponsor: Singapore-MIT Alliance

On the basis of the significant progresses in using implicit solvent models for studying DNA electrophoresis and other processes,^{5,14–16} efforts have recently been directed at the simulation of these and other systems of large number of solvent particles with explicit solvent.^{17–22} In particular, coarse-grained molecular dynamics (CG-MD) with explicit hydrodynamics has been used for studying the friction and the collision of polymers and the tethered polymers in shear flow,^{17–19} and the dissipative particle dynamics (DPD) method has been used for studying the mobility of DNA electrophoresis in a well-studied nano-fluidic device in explicit solvent.²²

Nonetheless, the computing cost of these explicit solvent methods tends to become prohibitively high for systems of very large number of solvent particles, primarily because of the need in computing pair-wise interactions among solvent particles by these methods.^{23,24} Therefore, it is desirable to explore other approaches capable of significantly reducing the cost for computing solvent–solvent interactions while maintaining sufficient level of simulation accuracy. One possible approach is the hybrid MD method that models intra-polymer and polymer-solvent interactions by MD and solvent–solvent interactions by simplified algorithms, which has been used in three forms. One combines MD with BD for simulating the particle Brownian motion.²⁵ The second combines MD with lattice Boltzmann for studying electrophoretic properties of highly charged colloids,^{26–28} and the third combines MD with mesoscale treatment of solvent–solvent interactions for studying solvent effect on polymer dynamics.^{20,29–31} By combining the advantages of the coarse-grained treatment in CG-MD^{17,18} and DPD²² with the efficient modeling of solvent–solvent interactions of the hybrid MD approach,^{23,24,26–28} we introduced and tested a new coarse-grained hybrid MD (CGH-MD) approach as a potentially useful method for complementing the more rigorous methods to simulate systems of larger number of solvent particles without substantially losing simulation accuracy.

In our method, both the polymer and the solvent are explicitly modeled at coarse grained level in a similar way as CG-MD^{17,18} and DPD.²² The bonding and excluded volume interactions between polymer beads are modeled by the finitely extensible nonlinear elastic potential (FENE) and Lennard-Jones potential,^{20,29–31} the excluded volume interaction between polymer bead and solvent are described by the Lennard-Jones potential, and the solvent-solvent interaction is represented by a frictional force and random force that obey the fluctuation-dissipation theorem.^{5,14,15,32} In this work, we tested whether the CGH-MD is capable of simulating a system of large number of particles in explicit solvent at substantially lower computing cost and at accuracy levels comparable to those of coarse-grained MD.^{17,18} Our method was first tested on the simulation of a standard linear polymer solution widely used in evaluating the performance of different computational methods.^{19,33} It was then tested on the computation of nonuniform distribution of ions in a cylindrical nanotube by comparing our result with that of CG-MD.^{33,34} Our method was further evaluated by using it to simulate the process of DNA electrophoresis in a polymer solution and in a well-studied nanofluidic device to compare its performance with observations and other simulation studies^{5,6} and to evaluate its computing cost with respect to those of other methods.

Method

We consider a standard bead-spring model of a polymer chain with N beads and assume that the polymer is placed in a solution with M mesoscopic solvent particles. Each polymer bead or solvent particle is considered as a sphere of radius r_p or r_s (typically van der Waals radii), respectively. Unless specific charge is explicitly added, each solvent particle is assumed to be neutral. This chain consists of N beads of mass m_b , and the neighboring beads are connected by an anharmonic spring represented by the FENE:

$$U_{\text{bond}}(r) = \begin{cases} -0.5\kappa R_0^2 \ln \left[1 - \left(\frac{r}{R_0} \right)^2 \right], & r \leq R_0 \\ \infty, & r > R_0 \end{cases} \quad (1)$$

where $R_0 = 1.5\sigma$ is an upper bound of the bead–bead bond distance, $\kappa = 30.0\epsilon/\sigma^2$ is a spring constant, σ and ϵ are the length and energy scale, and r is the distance between two connecting beads. The above parameters were appropriately chosen to model a self-avoiding chain.^{33,35} The excluded volume interactions for all bead–bead and bead–solvent interaction pairs in the system are given by the repulsive part of the Lennard-Jones (LJ) potential as follows

$$U_{\text{LJ}}(r) = \begin{cases} 4\epsilon \left[\left(\frac{r_0}{r} \right)^{12} - \left(\frac{r_0}{r} \right)^6 + \frac{1}{4} \right], & r \leq r_c \\ 0, & r > r_c \end{cases} \quad (2)$$

where $r_c = 2^{1/6} r_0$, $r_0 = r_p$ for bead–bead interaction, $r_0 = (r_s + r_p)/2$ for bead–solvent interaction. r_s , r_p are the van der Waals radii of polymer bead and solvent particle, respectively. Usually we set $r_s = \sigma$ and we can adjust the r_p to consider the size of the polymer bead.

The motion of the beads follows the Newton equation:

$$m_b \frac{d^2 \mathbf{R}_i}{dt^2} = -\nabla_{r_i} U_b + \mathbf{f}_{\text{ex}} \quad (i = 1, 2, \dots, N) \quad (3)$$

The potential $U_b = U_{\text{bond}} + U_{\text{b-b}} + U_{\text{b-s}}$ is the sum of the bond stretching potential U_{bond} , the excluded volume potential for the beads $U_{\text{b-b}}$, and an explicit term for the interaction between the beads and the solvent molecules $U_{\text{b-s}}$. The external force \mathbf{f}_{ex} arises from an external electric field acting on charged polymer beads and its dimensionless form is given by $\mathbf{f}_{\text{ex}} = (f_{\text{ex}}, 0, 0)$, where $f_{\text{ex}} = qE\sigma/k_B T$ and E is the electric field in the x -direction.

The motion of the i -th solvent particle is determined by the following equation:

$$m_s \frac{d^2 \mathbf{r}_i}{dt^2} = -\nabla_{r_i} U_{\text{b-s}} - \zeta_0 \left(\frac{d\mathbf{r}_i}{dt} - \langle \mathbf{v} \rangle \right) + \mathbf{f}_i(t) \quad (4)$$

m_s is the mass of a solvent particle, $U_{\text{b-s}}$ is the interaction between the beads and the solvent particles, and $-\zeta_0 \left(\frac{d\mathbf{r}_i}{dt} - \langle \mathbf{v} \rangle \right)$ is the frictional force between the solvent particle and its surrounding bulk solvent with an average velocity of $\langle \mathbf{v} \rangle$. In our work, the solvent particles as well as the polymer beads are treated at coarse-grained level. Therefore one can assume that there are a large number of water molecules in the

surrounding bulk to approximately estimate $\langle \mathbf{v} \rangle$. By using $\langle k_B T \rangle = \frac{m_s}{6(M-1)} \langle \sum_i \mathbf{v}_i^2 \rangle$ and central limit theorem, $\langle \mathbf{v} \rangle = \sqrt{\frac{6k_B T}{Mm_s}} \mathbf{v}_0$ in which \mathbf{v}_0 is a unit vector of random rotation in the range of 360° or 180° away from or at the inner planer surface of the solvent container.^{19,20,31} As $\langle \mathbf{v} \rangle$ is approximately given as a time-independent quantity, the friction coefficient ζ_0 can also be estimated by as a constant $\zeta_0 = m_b \tau^{-1}$.^{14,32,36} $\mathbf{f}_i(t)$ is the random force exerted by the surrounding solvent upon the i -th solvent particle, which is given in terms of the Gaussian white noise and obeys the fluctuation-dissipation theorem:

$$\langle \mathbf{f}_i(t) \rangle = 0, \quad \langle \mathbf{f}_i(t) \mathbf{f}_j(t') \rangle = 6k_B T \zeta_0 \delta_{ij} \delta(t - t'). \quad (5)$$

In the eqs. (4) and (5), the temperature T can be automatically controlled, the solvent friction is also included, and they can be considered as the extension of Langevin dynamics equation for the beads such that the energy, momentum as well as mass are conserved.^{5,14,15,36}

The particles (polymer beads and the solvent particles) in our method are coarse-grained. The mass of the polymer bead m_b is set as unit mass. We chose the dimensionless LJ unit throughout the article where the distances, energies, time, and temperature are measured in unit of σ , ϵ , $\tau = \zeta_0 \sigma^2 / \epsilon$,^{5,14} and ϵ / k_B , respectively. The neighbor-list method³⁷⁻³⁹ and leap-frog method^{14,15,40,41} were used in conducting CGH-MD simulation so as to achieve computational efficiency. The integration time step δt was set at 0.002–0.005 in unit of τ as suggested in the literature.^{17,18,42}

For the DNA chain, there is no heterogeneity in the DNA polymer and it is justified, because the distribution of G-C and A-T over every 150 base pairs is going to be the same; therefore the chemical composition of every segment along this coarse-grained DNA, on average, is the same. Based on the above condition, the exact values of the nondimensional unit quantities are chosen as: $\sigma = 50$ nm, $m_s = 0.85 m_b = 1.06 \times 10^{-19}$ kg, $\epsilon = k_B T = 4.11 \times 10^{-21}$ J, and $\tau = 2.76 \times 10^{-7}$ s. The average of physical quantities was computed from several separate simulation runs, each is of 10^6 – 10^7 time steps and is preceded by a common preliminary run of 10^3 time steps to eliminate possible dependence on the initial conformation. Average values from multiple runs were used for computing physical quantities to enhance statistical significance of simulation results. These algorithms and parameters were used for achieving sufficient computational accuracies in the simulation of systems of very large number of solvent particles, such as a self-avoiding polymer chain in solvents, DNA electrophoresis in a polymer solution and in a well-studied nanofluidic device.^{5,6}

Results and Discussion

Test of the Computational Accuracy and Efficiency of CGH-MD

CGH-MD was first tested by using it to conduct a 3D simulation of a standard bead-spring linear polymer solution in a cubic box, which has been widely used for evaluating the performance of different computational methods.^{19,33} This box contains a poly-

Table 1. Comparison of the Computational Efficiency for Simulating Polymer Solutions by Using CG-MD, CGH-MD, and BD Methods

Cases	CG-MD	CGH-MD	BD
$M = 7681, N = 304$ ^{54,55}	1	–	53
$M = 2.78 \times 10^4, N = 100^a$	1	10.58	109.57
$M = 2.78 \times 10^4, N = 50^a$	1	11.90	659.63
$M = 2.22 \times 10^5, N = 100^a$	1	25.456	7499.92

M is the number of the solvent particles and N is the number of the polymer beads.

^aCalculated on a single CPU Ix26-AMD64 machine.

mer of N beads ($N = 50, 100$) and M solvent particles ($M \approx 10^4 \sim 10^6$). By varying r_c of the Lennard-Jones potential in eq.(2) for the interaction between the polymer bead and the solvent U_{b-s} , one can study the polymer collapse and extension phenomena at different solvent conditions.¹⁹ In this work, r_c was chosen as two separate values at $r_c = 2^{1/6} \sigma$ (repulsive) and 3σ (attractive),^{43,44} which gives $R_g \sim N^\nu$ (R_g is the radius of gyration) with an exponent of $\nu \approx 0.338$ and 0.595 respectively. These computed values are 2.4% and 1.2% higher than the theoretical values of $\nu = 1/3$ and 0.588 respectively. For comparison, the computed values from a more rigorous simulation method are 2.0% higher and 1.4% lower than the theoretical values, respectively.¹⁹ Therefore, the accuracy level of our method appears to be quantitative close to that of more rigorous methods. In general, our simulation results are in good agreement with observations⁴⁵⁻⁴⁹ and the reported values from other more rigorous theoretical methods.^{19,33,50} Moreover, we also computed the diffusion coefficient of the solvents by using $D_s = \frac{1}{3M} \int_0^\infty \langle \sum_{j=1}^M \mathbf{v}_j(t) \cdot \mathbf{v}_j(0) \rangle dt$.^{17,51,52} The computed value of the diffusion coefficient is 0.061 ± 0.001 , which is also in agreement with the reported computational results.^{17,51-53} Therefore, CGH-MD appears to be capable of correctly predicting the physical properties of the polymer solution.

Table 1 gives the computational efficiency for CG-MD, CGH-MD, BD methods for simulating polymer solutions that contain various number of water particles, where the computational efficiency of corresponding CG-MD was assumed to one. Expectedly, BD gives far superior computational efficiency because of its implicit solvent treatment. However, this computationally efficient method is less useful for other systems with nonuniformly distributed electrostatic interactions, hydrophobic effects, and bound and sequestered water molecules. The computing time of CGH-MD and CG-MD is also displayed in Figure 1, which shows that the computing time of CGH-MD is one to multiple orders of magnitude shorter than that of CG-MD for simulating polymer solutions. All computing time was measured by the CPU time needed to complete 10^6 time steps. The computing time of CGH-MD linearly increases with the number of the solvent particles, M , while that of CG-MD is proportional to M^2 even though the use of distance cutoff helps reducing the computing cost to a fraction of M^2 .

The difference between the computing time of CGH-MD and that of CG-MD arises because of the extra need of the later in computing pair-wise interactions among all solvent particles at

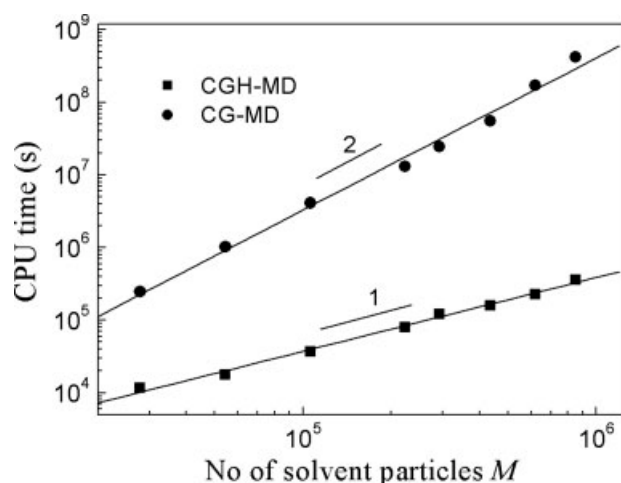


Figure 1. CPU time for simulating a polymer solution by using coarse-grained MD (spheres) and CGH-MD (squares) as a function of number of solvent particles M . The polymer is composed of $N = 100$ beads. The simulation is conducted on a single CPU lx26-AMD64 workstation.

$\sim 1\%$ of the time steps ($\sim 10^4$ times). In spite of the use of neighbor-list or/and the link-cell methods, the list or cell memberships needs to be regularly updated after every one hundred or so time steps, which necessitates the computation of $M^2/2$ pair-wise interactions among all the solvent particles for a total of $(10^6-10^7)/100$ times (total number of time steps divided by 100). In contrast, there is no need to compute pair-wise solvent-solvent interaction in CGH-MD, as solvent-solvent interactions are approximately represented by effective frictional and random forces, thereby significantly reducing the computing cost of CGH-MD without substantially reducing the computing accuracy.

Based on the actual computing costs of simulating polymer solutions and the knowledge, the computing costs of CGH-MD and CG-MD are proportional to M and M^2 , respectively, and CGH-MD appears to be capable of simulating systems of up to 10^7-10^8 water particles at speeds up to 10,000 times faster than CG-MD depending on the size of the system or the number of solvent particles. The computing cost of DPD (dissipative particle dynamics) is closer to that of coarse-grain MD than to CGH-MD, as it needs to compute pair-wise interactions among all of the coarse-grain solvent particles. To further estimate the comparative computing cost of CGH-MD against DPD, we used CGH-MD method to simulate the same system studied by DPD (simulation of DNA electrophoresis in a well-studied nanofluidic device).²² By comparing with the computing cost of DPD (obtained via personal communication with the author of the DPD work²² who developed the code and conducted relevant computational studies), we found that CGH-MD completed the same computing task 10–100 times faster than DPD.

Ion Distribution Pattern

To test the capability of CGH-MD in computing nonuniform distribution of solvent ions, we also computed the ion distribu-

tion inside a cylindrical nanotube and compared our result with that of MD.^{33,56} The radius and the length of the nanotube were chosen as 10 and 100σ , respectively, which were filled with 2.67×10^4 solvent particles with 1% and 1% of which assigned $+1$ charge and -1 charge, respectively. The electrostatic interaction between charged pairs was modeled by a truncated Coulomb interaction potential used in earlier MD simulations.^{33,39} Figure 2 shows our computed positive and negative ion distribution as a function of the distance to the walls of the nanotube in the equilibrium state. The distribution pattern is very similar to that of MD.^{33,56} There are significant amount of positive charges concentrated near the walls and higher level of negative charges distributed near the layer of positive charges. When the distance from the wall is larger than the $1.5\sigma_0$, the net charge is near zero. This suggests that CGH-MD is capable of computing non-uniform ion distributions at accuracy levels comparable to the more rigorous MD.^{33,56}

Application to DNA Electrophoresis in Polymer Solution Under a Steady Electric Field

CGH-MD was applied to the 3D simulation of DNA electrophoresis in a solution of cubic box ($L^3 = 64^3\sigma^3$, L is the width of the box). The box contains a DNA chain of length $N = 50$ (in unit of length scale σ) and 2.23×10^5 coarse-grained solvent particles under an external electric field with $f_{ex} = 2, 4, 8$. Figure 3 presents the snapshots of the chain conformations with $f_{ex} = 4$. For viewing clarity, only 1% of the solvent particles are explicitly shown in the figure. As shown in Figure 3a–3f, the DNA chain was found to adopt multiple conformations including the experimentally observed U-shape or V-shape conformation.^{3,57} U-shape or V-shape conformation has also been found in other simulation studies.^{14,15} Figure 4 shows the time development variation of the x component of the DNA end-to-end distance X_{end} and the maximum bead-bead distance within the DNA chain in the x direction X_{max} , respectively. A chain with a U-shape conformation has small X_{end}/N in comparison with X_{max}/N . But for the stretched chain, X_{end}/N has the similar value with

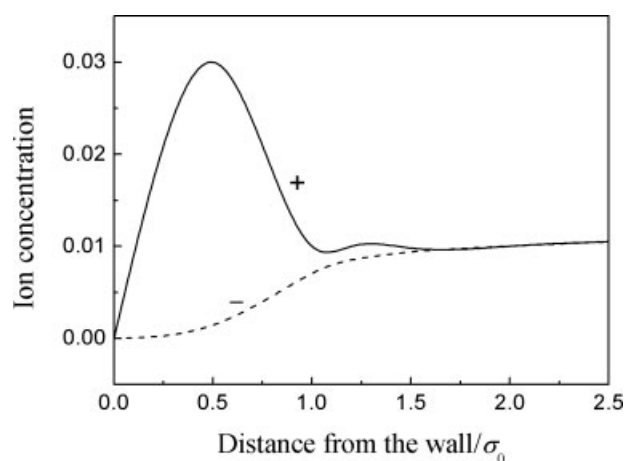


Figure 2. Distribution of positive (solid line) and negative (dashed line) ions near the wall of a cylindrical nanotube.

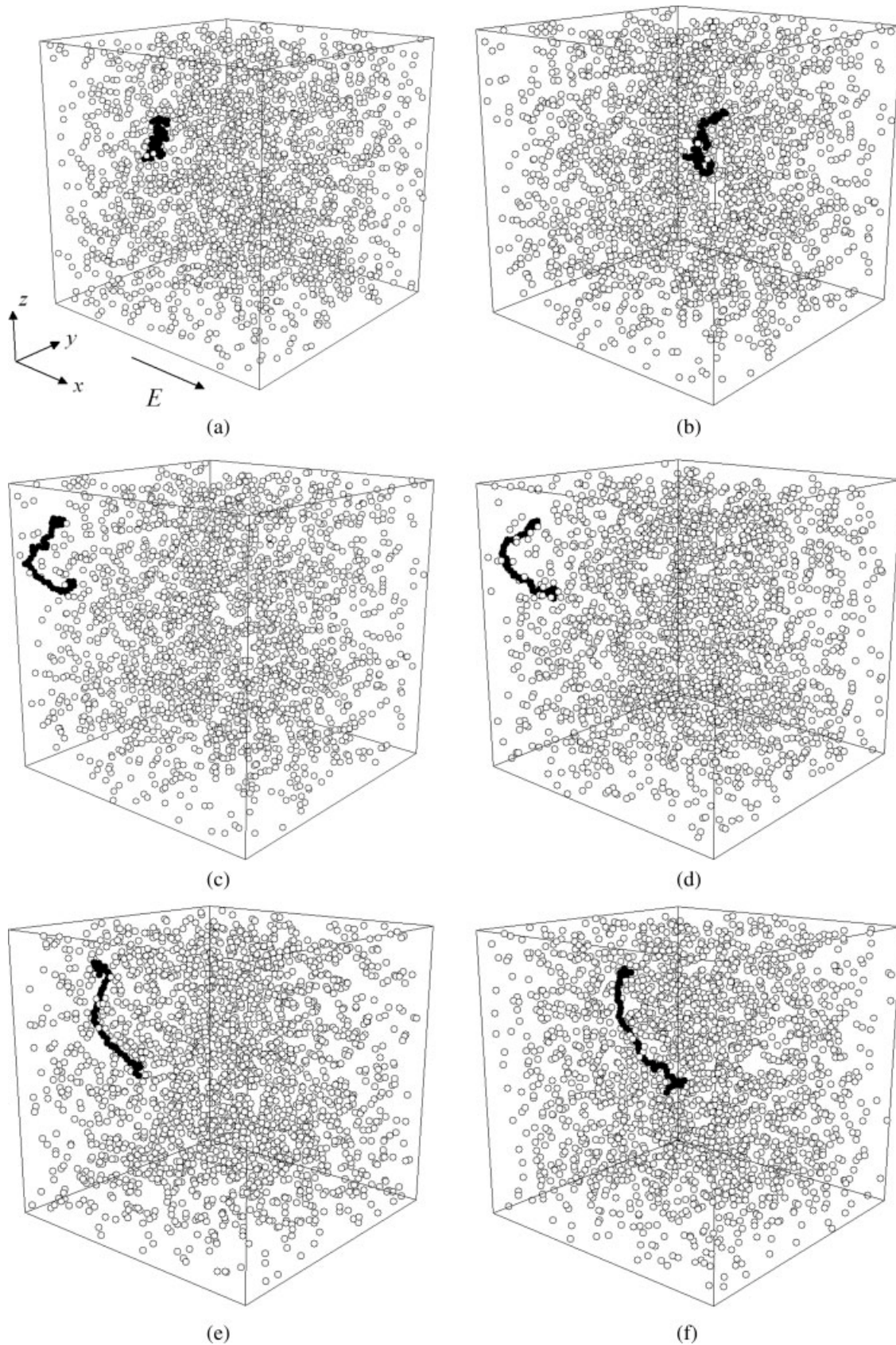


Figure 3. Snapshots of the chain conformations at the external force $f_{ex} = 4$ with $N = 50$. (a) $t = 10,000$, $X_c = 30.51$, (b) $t = 50,000$, $X_c = 55.70$, (c) $t = 70,000$, $X_c = 67.33$, (d) $t = 75,000$, $X_c = 70.29$, (e) $t = 100,000$, $X_c = 85.82$, and (f) $t = 130,000$, $X_c = 104.10$. X_c is x -position of the center-of-mass of the chain during the movement under the electric field.

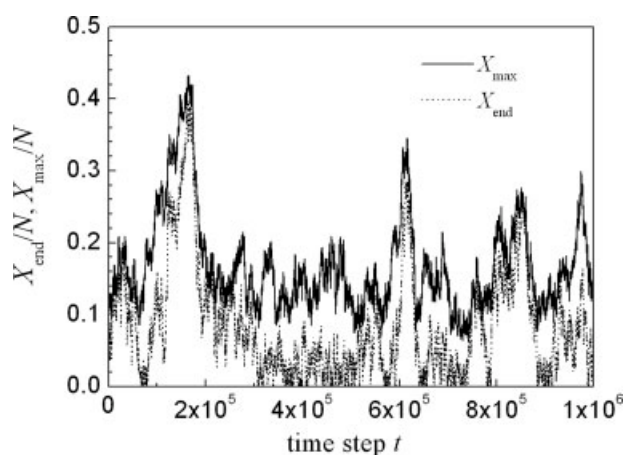


Figure 4. Polymer end-to-end distance X_{end} and the maximum length of a polymer chain along x -axis X_{max} as a function of time. The polymer is composed of $N = 50$ beads under an external force $f_{\text{ex}} = 4$.

X_{max}/N . It fluctuates between the elongated and compact states with no periodicity. These results are also in good agreement with other simulation results.^{14,15}

Figure 5 shows the movement of the center of the mass of DNA molecule as a function of time for $N = 50$ at different external fields with $f_{\text{ex}} = 2$ (solid line), 4 (dashed line), and 8 (dot line). The DNA chain was found to migrate along x -direction under the electric field. The higher the electric field, the faster the DNA chain migrates. The mobility μ ($\mu = v/E$, v is the velocity) as a function of chain length is given in Figure 6. As the chain length increases, the mobility decreases, but when the chain length is very large, the mobility is almost independent of the chain length. The independence of the chain length is also observed in experiment when using gel or polymer solutions and other models to study DNA electrophoresis.^{1,2}

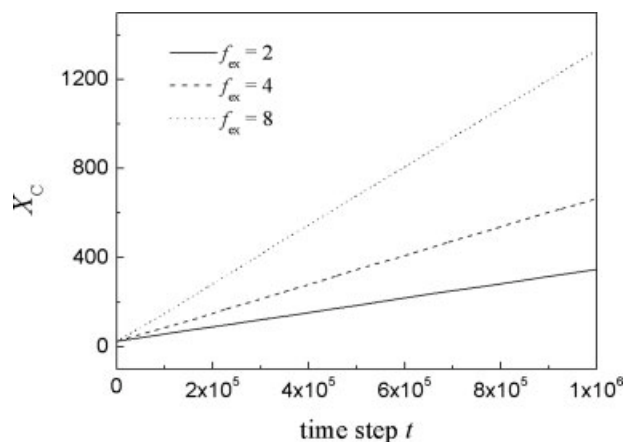


Figure 5. Center-of-mass X_c of a polymer for $N = 50$ beads at different external forces as a function of time. The external force is 2 (solid line), 4 (dashed line), and 8 (dot line).

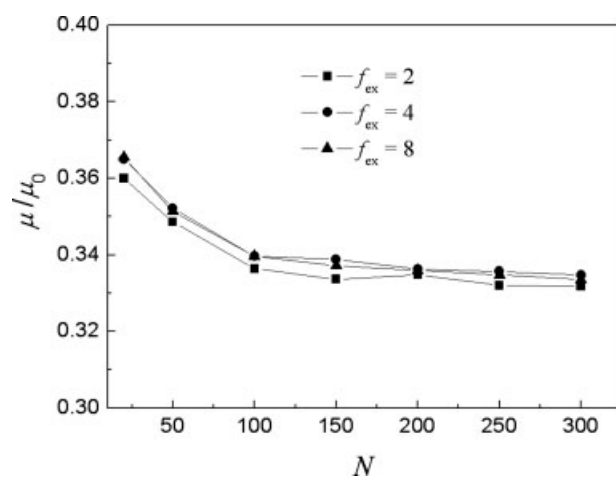


Figure 6. Relative mobility μ/μ_0 as a function of chain length N at different external fields $f_{\text{ex}} = 2$ (square), 4 (sphere), 8 (triangle).

Application to DNA Electrophoresis in a Well-Studied Nanofluidic Device

CGH-MD was further tested in the simulation of DNA electrophoresis in a well-studied nanofluidic device in 3D.^{8–10,58,59} This device is schematically shown in Figure 7. The lengths of one repeating unit of the channel along the x -direction and the y -direction are $L_x = 100 \sigma$ and $L_y = 50 \sigma$ (σ is comparable to the persistence length of the DNA chain, 50 nm, or about 150 bp.), respectively. The lengths of the deep and shallow regions of the channel, t_d and t_s , are 30σ and 3σ , respectively. The periodic boundary conditions were used along the x and y directions to mimic the effects of neighboring units. There are about 7×10^4 solvent particles in each unit. This work focused on the simulation of long DNA chain of length $N = 100$ (corresponding to 15 kbp). For comparison, the simulation results for DNA chain of $N = 50$ were also provided. The electric field is fixed at $E_{\text{av}}/E_0 = 5.5$ ($E_0 = k_B T / \sigma |q|$), which corresponds to the experimental value of $E \sim 95 \text{V/cm}$.⁵

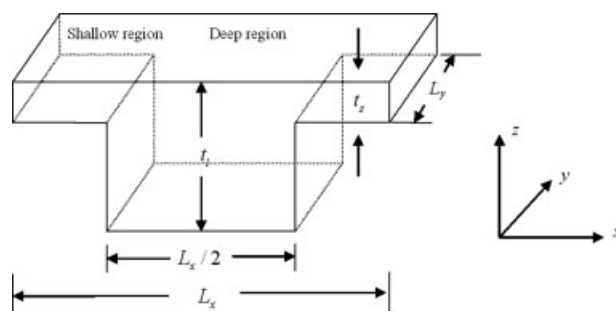


Figure 7. Schematic representation of the nanofluidic device. Only one repeated unit is shown. The lengths of the nanochannel, L_x , L_y , represent the repeated unit along the x - and y -direction, respectively. t_d and t_s are the lengths of the deep and shallow regions, respectively.

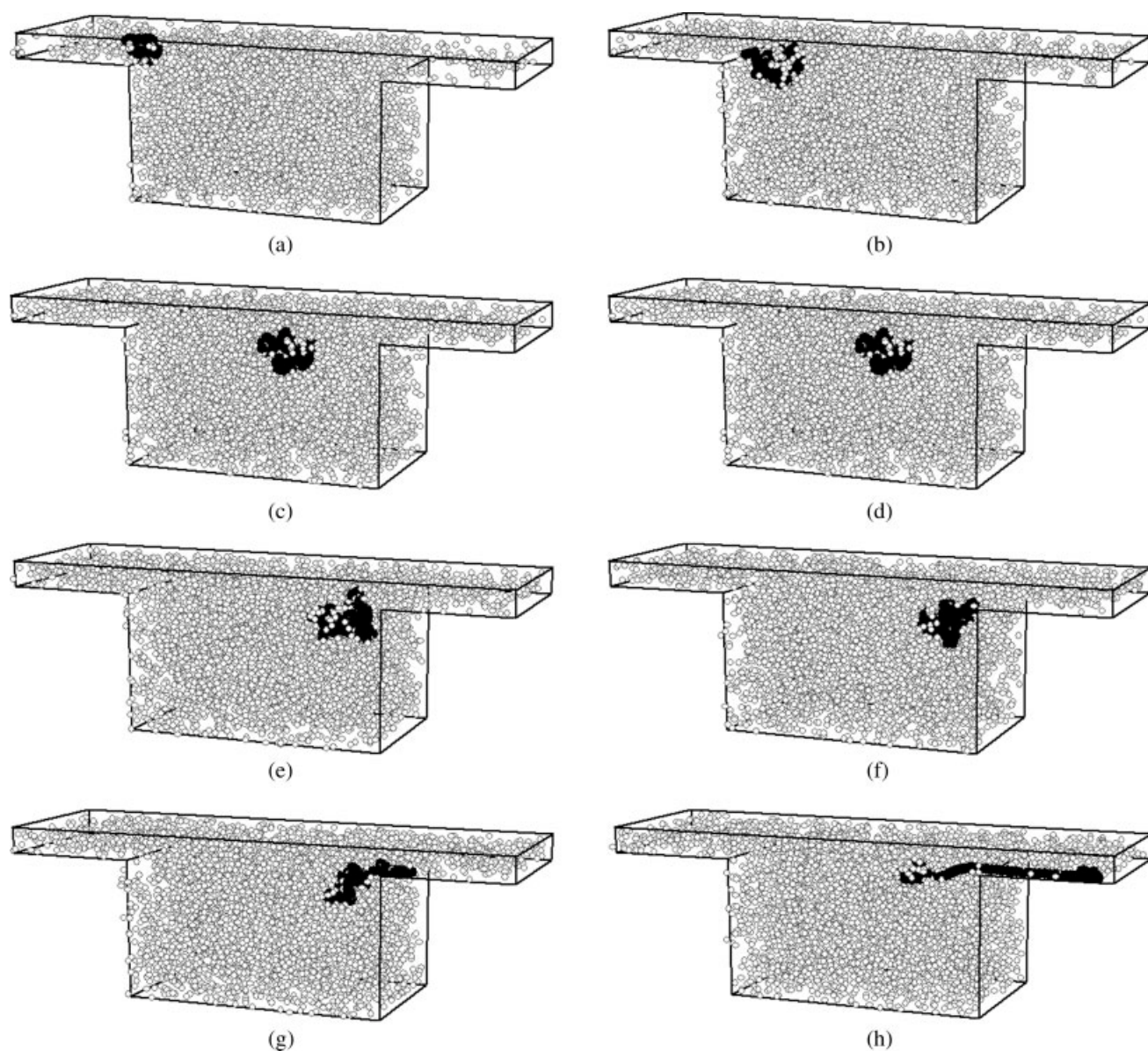


Figure 8. Snapshot of the movement of DNA chain in the nanofluidic device. Gray objects: solvent particles, black chain: DNA chain. (a) $t = 11,000$, $X_c = 24.00$, (b) $t = 44,000$, $X_c = 32.15$, (c) $t = 52,000$, $X_c = 34.44$, (d) $t = 190,000$, $X_c = 55.84$, (e) $t = 250,000$, $X_c = 61.10$, (f) $t = 273,000$, $X_c = 67.71$, (g) $t = 277,000$, $X_c = 68.16$, and (h) $t = 282,000$, $X_c = 71.59$.

Figure 8 shows the snapshots of the simulated DNA conformation at different locations of the nanofluidic device. For viewing clarity, only 10% of the solvent particles in the region of $20\sigma < y < 50\sigma$ are explicitly shown. As the DNA moves from the shallow region to the deep one, it adopts increasingly more extended random coil conformation with a higher entropy, which can be seen from Figure 8a–c. At the interface between the deep and shallow regions, it takes significantly longer time for the head of the DNA to enter the shallow region due to the primarily unfavorable entropic reduction. After its head enters into the shallow region (Figure 8f), the whole DNA promptly passes through the shallow

region as a stretched chain. The position of the leading bead (X_{lead}), the ending bead (X_{end}), and the center-of-mass (X_c) of the DNA as a function of time are shown in Figure 9. The DNA chain appears to move faster in the shallow region than in the deep region, and the ending bead moves backward slightly with respect to its head. This is an expected behavior, because when it enters the boundary between the deep and shallow regions, the chain has to tailor its conformation under the electric field in such a way that its leading bead can enter the shallow region.

The x -position of the leading bead, the ending bead, and the center-of-mass of the DNA chain of as a function of time are

also shown in Figure 9. To clearly see the DNA movement in the channel along the x -direction, we give x -positions of the DNA chain in more than one periodic nanochannel ($y > L_x$). Comparing with Figure 9a and 9b, it can be easily seen that it takes longer time for the leading bead of shorter DNA chain to enter the shallow region. These results are consistent with observations and are comparable to those of other simulation studies.^{5,6,8–10} The mobility of DNA chains of lengths $N = 100$ and 50 as a function of the electric field is shown in Figure 10. The computed mobility of these DNA chains increases with increasing electric field and saturates at higher electric field. The longer chain shows higher mobility than the shorter one. These results

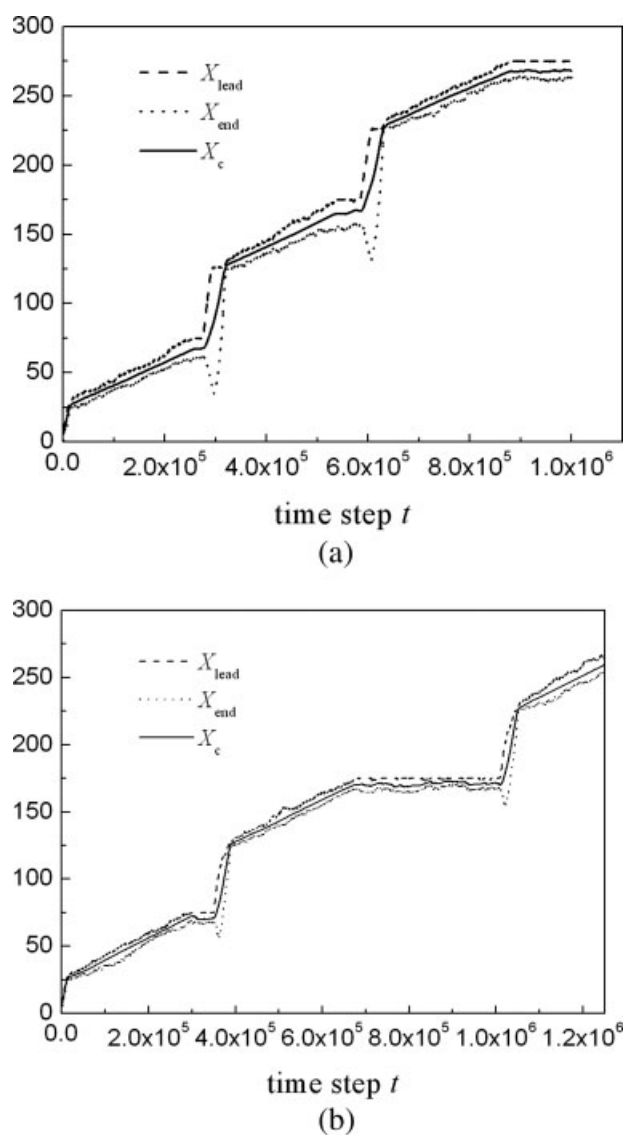


Figure 9. X -component of the displacement of the leading bead (dashed line), ending bead (dot line), and center-of-mass (solid line) of the DNA chain as a function of time. The DNA chain is composed of (a) $N = 100$ and (b) $N = 50$ beads.

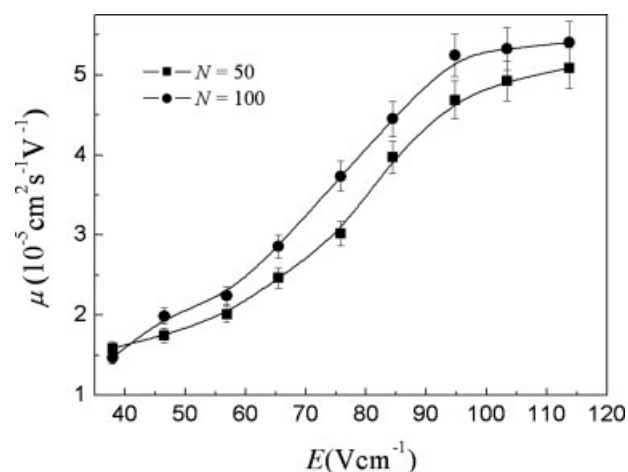


Figure 10. Mobility of a DNA chain in the nanofluidic device.

are consistent with observations and in qualitative agreement with those of other simulation studies.^{5,6,8}

Conclusion

CGH-MD showed comparatively good performance in simulating a typical polymer solution, ion distribution in a nanotube, and DNA electrophoresis in polymer solutions and in a nanofluidic device at significantly lower computing cost than those of more rigorous methods. As a computationally efficient explicit-solvent method, CGH-MD is potentially useful for simulating systems of large number of water particles to complement more rigorous methods. It may also be applied to the study of polar and hydrophobic effects,¹³ nonuniformly distributed electrostatic interactions, and the effects associated with bound and sequestered water molecules^{12,13} in various bio-macromolecular and nanofluidic systems such as the electrophoresis of DNA,³⁶ proteins,⁶⁰ viral particles, and complexes⁶¹ in nanofluidic,^{34,58,59,62} microfluidic,^{63,64} and microstructure array^{16,65} systems.

Acknowledgments

The authors thank Prof. B. W. Li and Prof. H. J. Yang for their useful discussion of the numerical method.

References

- Heller, C. Analysis of Nucleic Acid by Capillary Electrophoresis; Vieweg Verlagsgesellschaft: Wiesbaden, 1997.
- Viovy, J. L. Rev Mod Phys 2000, 72, 813.
- Ueda, M.; Oana, H.; Baba, Y.; Doi, M.; Yoshikawa, K. Biophys Chem 1998, 71, 113–123.
- Smith, S. B.; Aldridge, P. K.; Callis, J. B. Science 1989, 243, 203.
- Streek, M.; Schmid, F.; Duong, T. T.; Ros, A. J Biotechnol 2004, 112, 79.
- Tessier, F.; Labrie, J.; Slater, G. W. Macromolecules 2002, 35, 4791.

7. Panwar, A. S.; Kumar, S. *Macromolecules* 2006, 39, 1279.
8. Han, J.; Turner, S. W.; Craighead, H. G. *Phys Rev Lett* 1999, 83, 1688.
9. Han, J.; Craighead, H. G. *Science* 2000, 288, 1026.
10. Han, J.; Turner, S. W.; Craighead, H. G. *Phys Rev Lett* 2001, 86, 1394.
11. Han, J. Y.; Craighead, H. G. *Anal Chem* 2002, 74, 394.
12. Levy, R. M.; Gallicchio, E. *Annu Rev Phys Chem* 1998, 49, 531.
13. Gilson, M. K.; Zhou, H. X. *Annu Rev Biophys Biomol Struct* 2007, 36, 21.
14. Noguchi, H. *J Chem Phys* 2000, 112, 9671.
15. Noguchi, H.; Takasu, M. *J Chem Phys* 2001, 114, 7260.
16. Maleki-Jirsaraei, N.; Sarbolouki, M.-N.; Rouhani, S. *Electrophoresis* 2007, 28, 301.
17. Kenward, M.; Slater, G. W. *Eur Phys J E* 2004, 14, 55.
18. Kenward, M.; Slater, G. W. *Eur Phys J E* 2006, 20, 125.
19. Lee, S. H.; Kapral, R. *J Chem Phys* 2006, 124, 214901.
20. Lee, S. H.; Kapral, R. *J Chem Phys* 2004, 121, 11163.
21. Gratton, Y.; Slater, G. W. *Eur Phys J E* 2005, 17, 455.
22. Duong-Hong, D.; Wang, J. S.; Liu, G. R.; Chen, Y. Z.; Han, J.; Hadjiconstantinou, N. G. *Microfluid Nanofluid* 2007, 3, DOI:10.1007/s10404-10007-10170-10407.
23. Hoogerbrugge, P. J.; Koelman, J. *Europhys Lett* 1992, 19, 155.
24. Groot, R. D.; Warren, P. B. *J Chem Phys* 1997, 107, 4423.
25. Chen, J. C.; Kim, A. S. *Adv Colloid Interface Sci* 2004, 112, 159.
26. Chatterji, A.; Horbach, J. *J Chem Phys* 2005, 122, 184903.
27. Chatterji, A.; Horbach, J. *Math Comput Simul* 2006, 72, 98.
28. Chatterji, A.; Horbach, J. *J Chem Phys* 2007, 126, 064907.
29. Lee, S. H.; Kapral, R. *J Chem Phys* 2006, 124, 214901.
30. Sergi, A.; Kapral, R.; Pomes, R. *Biophys J* 2002, 82, 520A.
31. Malevanets, A.; Kapral, R. *J Chem Phys* 2000, 112, 7260.
32. Ou, Z. Y.; Muthukumar, M. *J Chem Phys* 2006, 124, 154902.
33. Tessier, F.; Slater, G. W. *Macromolecules* 2006, 39, 1250.
34. Fu, J. P.; Schoch, R. B.; Stevens, A. L.; Tannenbaum, S. R.; Han, J. *Y. Nat Nanotechnol* 2007, 2, 121.
35. Kremer, K.; Grest, G. S. *J Chem Phys* 1990, 92, 5057.
36. Luo, H. B.; Gersappe, D. *Electrophoresis* 2002, 23, 2690.
37. Verlet, L. *Phys Rev* 1967, 159, 98.
38. Ralston, B. J.; Fincham, D. *Comput Phys Commun* 1981, 23, 127.
39. Allen, M. P.; Tildesley, D. J. *Computer Simulation of Liquids*; Oxford University Press: New York, 1987.
40. Mazur, A. K. *J Comput Phys* 1997, 136, 354.
41. Hockney, R. W.; Eastwood, J. W. *Computer Simulation Using Particles*; McGraw-Hill: New York, 1981.
42. Muthukumar, M.; Kong, C. Y. *Proc Natl Acad Sci USA* 2006, 103, 5273.
43. Gottberg, F. K.; Smith, K. A.; Hatton, T. A. *J Chem Phys* 1997, 106, 9850.
44. Huh, J.; Kim, K. H.; Ahn, C. H.; Jo, W. H. *J Chem Phys* 2004, 121, 4998.
45. Berry, G. C. *J Chem Phys* 1966, 44, 4550.
46. Bantle, S.; Schmidt, M.; Burchard, W. *Macromolecules* 1982, 15, 1604.
47. Einaga, Y.; Abe, F.; Yamakawa, H. *Macromolecules* 1993, 26, 6243.
48. Appelt, B.; Meyerhoff, G. *Macromolecules* 1980, 13, 657.
49. Huber, K.; Bantle, S.; Lutz, P.; Burchard, W. *Macromolecules* 1985, 18, 1461.
50. de Gennes, P. G. *Scaling Concepts in Polymer Physics*; Cornell University Press: Ithaca, 1988.
51. Bazhenov, A. M.; Heyes, D. M. *J Chem Phys* 1990, 92, 1106.
52. Meier, K.; Laesecke, A.; Kabelac, S. *J Chem Phys* 2004, 121, 9526.
53. Levesque, D.; Verlet, L. *Phys Rev A* 1970, 2, 2514.
54. Ando, T.; Meguro, U.; Yamata, I. *J Comput Chem Jpn* 2002, 1, 115.
55. Ando, T.; Meguro, U.; Yamata, I. *J Comput Chem Jpn* 2004, 3, 129.
56. Qiao, R. *Langmuir* 2006, 22, 7096.
57. Shi, X. L.; Hammond, R. W.; Morris, M. D. *Anal Chem* 1995, 67, 1132.
58. Fu, J. P.; Mao, P.; Han, J. Y. *Appl Phys Lett* 2005, 87, 263902.
59. Fu, J. P.; Yoo, J.; Han, J. Y. *Phys Rev Lett* 2006, 97, 018103.
60. Marengo, E.; Robotti, E.; Gianotti, V.; Righetti, P. G.; Cecconi, D.; Domenici, E. *Electrophoresis* 2003, 24, 225.
61. Kremser, L.; NBilek, G.; Blaas, D.; Kenndler, E. *J Sep Sci* 2007, 30, 1704.
62. Kim, S. J.; Wang, Y.-C.; Lee, J. H.; Jang, H.; Han, J. *Phys Rev Lett* 2007, 99, 044501.
63. Jendrejack, R. M.; Schwartz, D. C.; Graham, M. D.; de Pablo, J. J. *J Chem Phys* 2003, 119, 1165.
64. Chen, Y.-L.; Graham, M. D.; de Pablo, J. J.; Jo, K.; Schwartz, D. C. *Macromolecules* 2005, 38, 6680.
65. Dorfman, K. D. *Phys Rev E* 2006, 73, 061922.